Nature of α and β Particles in Glycogen Using Molecular Size Distributions

ARTICLE *in* BIOMACROMOLECULES · MARCH 2010

Impact Factor: 5.75 · DOI: 10.1021/bm100074p · Source: PubMed

6 AUTHORS, INCLUDING:

Mitchell A Sullivan
SickKids
14 PUBLICATIONS **117** CITATIONS
SEE PROFILE

Francisco Vilaplana
KTH Royal Institute of Technology
47 PUBLICATIONS **964** CITATIONS
SEE PROFILE

David Stapleton
University of Melbourne
91 PUBLICATIONS **6,114** CITATIONS
SEE PROFILE

Nature of α and β Particles in Glycogen Using Molecular Size Distributions

Mitchell A. Sullivan,[†] Francisco Vilaplana,[†] Richard A. Cave,[†] David Stapleton,[‡] Angus A. Gray-Weale,[§] and Robert G. Gilbert*,[†]

Department of Biochemistry and Molecular Biology, Bio21 Molecular Science and Biotechnology Institute, The University of Melbourne, Victoria, Australia, School of Chemistry, Monash University, Victoria 3800, Australia, and CNAFS and LCAFS, Hartley Teakle Building, University of Queensland, Brisbane, Qld 4072, Australia

Received January 21, 2010; Revised Manuscript Received February 19, 2010

Glycogen is a randomly hyperbranched glucose polymer. Complex branched polymers have two structural levels: individual branches and the way these branches are linked. Liver glycogen has a third level: supramolecular clusters of β particles which form larger clusters of α particles. Size distributions of native glycogen were characterized using size exclusion chromatography (SEC) to find the number and weight distributions and the size dependences of the number- and weight-average masses. These were fitted to two distinct randomly joined reference structures, constructed by random attachment of individual branches and as random aggregates of β particles. The *z*-average size of the α particles in dimethylsulfoxide does not change significantly with high concentrations of LiBr, a solvent system that would disrupt hydrogen bonding. These data reveal that the β particles are covalently bonded to form α particles through a hitherto unsuspected enzyme process, operative in the liver on particles above a certain size range.

Introduction

Glycogen, a hyperbranched glucose polymer, is a key energy reserve for animals (including humans). The cells with the biggest stores of glycogen are in the liver and skeletal muscle; other glycogen-containing cells include the brain, heart, skin, and adipose tissues.[1] Liver glycogen is quickly broken down in times of fasting, playing an important role in blood glucose homeostasis.[2] Glycogen's structure contains clues to its biosynthesis, regulation, and degradation. The branched nature of glycogen structure makes it hard to characterize. A full description of the branched structure of a polymer requires an infinitely hierarchical distribution function,[3] but useful information can be gleaned from three one-dimensional functions, which are various projections of this infinite-dimensional one: the number and weight distributions as a function of size and the dependence of the weight-average molecular weight, $\bar{M}_w$, on size. These are obtained experimentally by size separation of a sample using size-exclusion chromatography (SEC, also called gel-permeation chromatography, GPC) or field-flow fractionation.[4] The two distributions and the $\bar{M}_w$ size dependence are obtained, respectively, by viscometry,[3] differential refractive index (DRI), and multiangle laser light scattering (MALLS) detection.

The structure of a complex branched molecule in solution can be described at two levels: that of the individual branches (e.g., rat liver glycogen has an average chain length of 11 glucose residues with 9% branching[1]) and then, at a second level, as the way that these branches are joined together. However, liver glycogen has a special feature that is not seen in other complex branched polymers; transmission electron microscopy (TEM) suggests that there can be two levels of structure in isolated glycogen molecules, with the subunits known as α and β particles.[1,5,6] The β particles have diameters varying between 10 and 30 nm, while in mammalian liver cells, TEM suggests that the β particles adhere, forming large supermolecular complexes known as α particles, or α rosettes, which can have diameters as large as 300 nm (see Figure 1).[7,8] A sketch of the different structural levels is given in Figure 2.

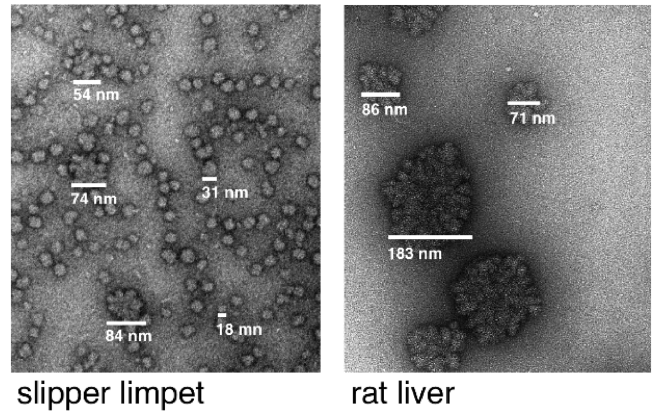

Figure 1. Transmission electron microscope images of slipper limpet (left) and rat liver (right) glycogens: β particles have diameters of ~20 nm and α particles are ~100 nm in diameter.

The question arises as to the nature and biosynthetic origin of these two types of subparticles, and also what might be the biological function of such an arrangement. Glycogen particles in cells contain not only glycogen, but also several bound proteins that are involved in glycogen metabolism, such as glycogen phosphorylase and glycogen synthase.[9] Glycogen synthesis is initiated by glycogenin, an autocatalytic enzyme that adds glucose from UDP-glucose on tyrosine-194 followed by the addition of approximately seven more glucose residues.[10,11]

* To whom correspondence should be addressed. E-mail: b.gilbert@uq.edu.au..
[†] University of Queensland.
[‡] The University of Melbourne.
[§] Monash University.

10.1021/bm100074p
Published on Web 03/02/2010

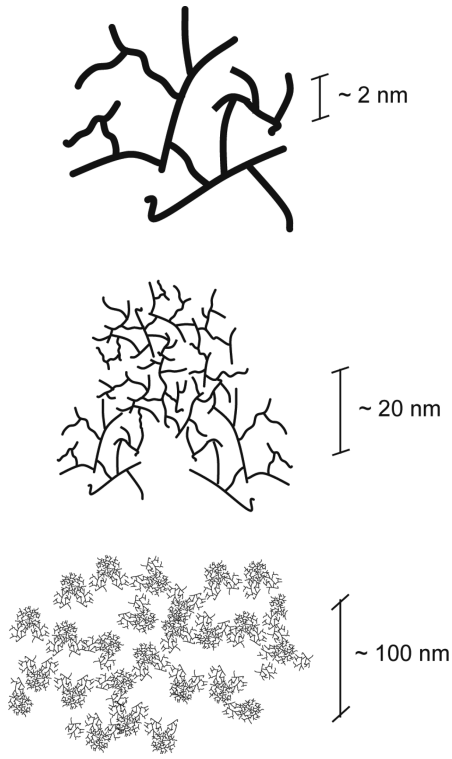

Figure 2. Sketch of the three structural levels in glycogen molecules in solution: (a) randomly joined branches, which on a larger scale form β particles (b), which in turn are joined on a larger scale to form α particles (c).

This protein-bound malto-oligosaccharide serves as a primer for glycogen synthase and glycogen-branching enzyme that catalyze the formation of α-(1,4) and α-(1,6) glycosidic linkages, respectively. It has been suggested that glycogen is organized into concentric tiers.[9] It is not apparent that any or some of these enzymatic processes have some additional function to form these two levels of high-order structure, if these were in fact covalently bonded. There is alternatively the possibility that β particles adhere to form α particles by hydrogen bonding and/or through protein−protein interactions.[12] The latter would be some combination of weak electrostatic and hydrogen bonding. Iwasama et al. tried unsuccessfully to separate liver β particles from each other with strong acid or reducing agent.[13]

We here use the detailed information available from triple-detector SEC to build a quantitative model of the structure of rat liver α particles. We study samples that are representative of in vivo glycogen molecules. It has been shown that commercially available glycogen particles (such as rabbit and bovine glycogen) often show significant degradation.[1] The reason for this degradation is a preparation that includes boiling. We use carefully extracted rat liver glycogen and, therefore, report the first full structural characterization of undegraded native glycogen. For comparison, the glycogen from the sea snail *Crepidula fornicata*, also known as the slipper limpet, has also been analyzed. This is an appropriate reference for commercially prepared glycogen because it is the least degraded.[1]

One way of obtaining useful information on a branched polymer's structure from size-distribution data involves computationally generating hypothetical polymer structures by the random assembly of certain components, denoted "simple units".[14−16] These simple units are usually linear chains chosen to have the same distribution of lengths as those present in the real polymer, and this is used to simulate the β particles. Here we also use a hypothetical structure for the α particles made by random assembly of β particles of glycogen. In both cases, any differences between experimental data and these random reference structures reveal the effects of structural correlations in the real polymer.

Because it is of interest if the β particles are attached by hydrogen bonding or electrostatic attraction to form α particles, or if there is a covalent attachment involved, the size was also examined in a solvent system that should disrupt any H bonding: DMSO with increasing concentrations of LiBr.

Experimental Section

Glycogen Purification. The livers from 8-week-old, random-fed, Sprague−Dawley rats were homogenized in five volumes of glycogen isolation buffer (50 mM Tris, pH 8, 150 mM NaCl, 2 mM EDTA, 50 mM NaF, 5 mM sodium pyrophosphate, and mini-complete protease inhibitors (Roche Applied Science, Indianapolis, IN)). This was centrifuged at 6000 *g* for 10 min at 4 °C. The resultant supernatant was centrifuged at 50000 *g* for 30 min. The pellet was resuspended in 1.5 mL of glycogen isolation buffer and layered over a 22.5 mL, stepwise sucrose gradient (25%, 50% and 75% in glycogen isolation buffer). This was centrifuged at 300 000 *g* for 2 h. The glycogen fraction pelleted through all three layers while the microsomal layer remained in the 25−50% sucrose fraction. The pellet was resuspended into 300 μL of glycogen isolation buffer and further resolved by application to a 35 mL, S500 (GE Healthcare) gel filtration column equilibrated in glycogen isolation buffer, chromatographed at 0.5 mL min^{-1}, and 1 min fractions collected. All animal experiments have been performed in compliance with the University of Melbourne ethics committee.

Dissolution of Glycogen. Purified rat liver glycogen was directly dissolved in the SEC eluent of dimethylsulfoxide (DMSO; HPLC grade, Sigma-Aldrich) with 0.5 wt % LiBr (ReagentPlus) at glycogen concentrations of 2 g L^{-1}.

SEC of Glycogen. Size separation here is performed by SEC in dimethylsulfoxide (DMSO) and LiBr as eluent, a solvent system that completely dissolves starch[17] and, thus, by inference, also glycogen. Shear scission can readily occur with large molecules during SEC separation, but fortunately, the size range above which shear scission occurs in the system used here[18] is larger than most glycogen molecules. There is experimental evidence[19−22] that SEC separates polymer molecules based on a size parameter that is proportional to the product of intrinsic viscosity and number-average molecule weight: the hydrodynamic volume V_h (although recent theoretical developments[23] suggest that alternative parameters such as span dimension might be considered as alternatives). V_h is defined by IUPAC as "the volume of a hydrodynamically equivalent sphere".[24] For convenience, data are presented in terms of hydrodynamic radius, R_h, with $V_h = {}^4/_3\pi R_h^3$. It is important to recall that SEC separation is by size, not by molecular weight; the size and molecular weight of a polymer are uniquely related only if the polymer is linear (unbranched).

Samples were injected into an Agilent 1100 Series SEC system (PSS GmbH. Mainz, Germany) using a GRAM preColumn, 30 and 3000 columns (PSS GmbH. Mainz, Germany) in series, in a column oven at 80 °C at a flow rate of 0.3 mL min^{-1}. The system was equipped with multiangle laser light scattering (MALLS; BIC-M_wA7000, Brookhaven Instrument Corp., New York, U.S.A.) detection, followed by parallel flow into a refractive index detector (RID; Shimadzu RID-10A, Shimadzu Corp., Japan) and a viscometric detector (ETA-2010, PSS GmbH, Mainz, Germany).

Pullulan standards (PSS GmbH, Mainz, Germany), with a molecular weight range of 342 to 1.66×10^6 Da, were dissolved directly into eluent and run through the system to generate a universal calibration curve, allowing the determination of the hydrodynamic volume from elution volume. The Mark−Houwink parameters for pullulan in DMSO/LiBr (0.5 wt %) at 80 °C are $K = 2.427 \times 10^{-4}$ dL g^{-1} and $a = 0.6804$ (Kramer and Kilz, PSS, Mainz, private communication). The upper

limit of R_h for the pullulan standards in this solvent is 52 nm. While the calibration curve can be extrapolated to higher values of R_h, in the type of system used here, this extrapolation is very sensitive to the calibration curve, and slight experimental scatter can cause large changes in apparent R_h beyond the range of the standards used.[18] Fortunately, for the present glycogen samples, most molecules have sizes below this upper calibration value. The value of the differential refractive index for glycogen in this system was taken to be the same as rice starch (measured by PSS, Mainz), $dn/dc = 0.0544$ mL g^{-1}; that starch was mainly amylopectin, whose branching structure is similar in many ways to that of glycogen.

The quantities obtained here from multidetector SEC are the number distribution $N(V_h)$, the SEC weight distribution $w(\log V_h)$, and the V_h dependence of the weight-average molecular weight, $\bar{M}_w(V_h)$; these in turn yield the V_h dependence of the number-average molecular weight, $\bar{M}_n(V_h)$. These quantities are obtained from the signals from the three detectors using conventional methods, except for $N(V_h)$ and $\bar{M}_n(V_h)$, which were obtained using an expression given elsewhere:[3]

$$N(V_h) = \frac{S_{visc}(t_{el})}{V_h^2} \frac{d\,\tilde{t}_{el}(V_h)}{d \log V_h} \quad (1)$$

$$\bar{M}_n(V_h) = \frac{5}{2} \frac{V_h N_A}{[\eta]} \quad (2)$$

Here $S_{visc}(t_{el})$ is the signal from the viscometric detector at elution time t_{el}, providing this signal is proportional to the specific viscosity (a slight correction should be used for other types of signal), $\tilde{t}_{el}(V_h)$ is the elution time as a function of hydrodynamic volume, that is, the inverse of the calibration curve, N_A is the Avogadro constant, and $[\eta]$ the intrinsic viscosity at that elution time (obtained directly from $S_{visc}(t_{el})$, which for the instrument and software used here is the specific viscosity).

Average Particle Size. Samples of rat liver glycogen were dissolved in DMSO/LiBr (0.1 wt % w/w glycogen/solvent) with varying concentrations of LiBr at 0, 0.5, and 5 wt %. The *z*-average particle diameter was then determined using dynamic light scattering with a Zetasizer Nano (Malvern Instruments, Malvern, U.K.). DMSO/LiBr is effective at breaking up such noncovalent links: for example, it is able to completely dissolve high-amylose starch (with strong noncovalent inter- and intrachain interactions) under mild conditions with 5% LiBr.[17] If the interaction causing formation of α particles were noncovalent, then the average size would change from ~150 to ~20 nm. To test this, average sizes were obtained using dynamic light scattering, which is very sensitive to larger particles. When SEC is used to obtain accurate size distributions in such a high concentration of LiBr, it poses considerable technical difficulties, but fortunately, the requisite information can be obtained from the average size from light scattering, where the technical problems are not severe.

Theory

The comparison of experiment and theory may take one of two forms, as follows. The first form involves comparison of the size versus mass dependence of the real polymer to that of the randomly branched reference structures. In the examples given here, this takes the form of a hydrodynamic radius dependence of the weight-average molecular weight of polymers with that radius. This method most clearly shows changes in architecture with polymer size but reveals no information about the numbers of polymers of different sizes. The second approach compares a hypothetical randomly branched weight distribution to the actual weight distribution.[14,16] The randomly branched reference weight distribution is found from the experimental number distribution and the theoretical mass versus size curve. The degree of randomness can be inferred from the real and hypothetical distributions, with truly randomly branched polymers showing agreement in the two distributions. If, however, both distributions are different, then a more complex structure must be sought.

Although the randomly branched reference structure is not intended as a model for biosynthesis, it does provide a convenient reference, allowing the uncovering of some biosynthetic properties. For instance, molecules that show a significant difference between real and hypothetical distributions are more likely to involve a synthetic route with higher complexity than a polymer with real distributions that resemble the hypothetical random reference structure.

Erlander and French considered in their classic work[25−27] on glycogen and amylopectin the random assembly of a hyperbranched polymer, with particular attention to the molecular weight distribution, degrees of polymerization, and dispersity. Our approach is similar in that we consider random assembly, but we add a description of the distribution in space of the polymers' mass. Also, we do not regard our model as a model for synthesis. The experiments we report here are based on separation by, or measurement of, the hydrodynamic volumes of the polymers, and so we need a theory that describes the spatial arrangement of a polymer's mass.

Constructing the Reference Structures. The method for generating a reference randomly hyperbranched structure, Random Branching Theory (RBT), has been described in detail elsewhere.[15,16] Here we briefly outline the method, concentrating on those features that have not previously been used.

We compare our experimental data to predictions based on a randomly assembled reference structure generated using RBT. Both methods of making this comparison require an RBT estimate of the relation between the radii of gyration of the polymers and their masses. The radius of gyration R_g can be measured experimentally for glycogen using MALLS, but is found to be quite close to R_h.[28] The difference between R_h and R_g is sufficiently small that they are taken to be the same for the present purposes. It is not unusual for highly branched species, with roughly spherical density distributions, to have similar values of the hydrodynamic and gyration radii. For example, high generation dendrimers, of roughly the same size as the beta particles of glycogen we discuss below, have a hydrodynamic radius only slightly higher than their radius of gyration.[29]

To generate the randomly branched reference structure, first the sizes of the simple units that are to be randomly attached need to be specified. RBT may be used with a variety of simple units, so named because they usually have a structure simpler than the overall polymer. The linear chains from which a branched glycogen polymer is constructed contain from 7 to 13 glucose monomers.[1] The simplest application of the method is to attach these linear chains to each other at random. We take this approach below and also consider a larger scale structure: the assembly of α particles by the random attachment of β particles to each other. We then need two randomly branched reference structures: that obtained by random assembly of short linear chains, and that obtained by random assembly of β particles. In both cases, X denotes the number of monomers in the simple unit.

It is assumed that all simple units possess a Gaussian density profile. If the simple unit is a linear polymer, then the form for $\sigma(X)$, the width of the profile, is the same as used previously.[16] If the simple unit is a β particle, we must use a different relation for $\sigma(X)$. For want of better knowledge of the internal structure of a β particle, we assume it to have a Gaussian density profile

and that the particle's volume is proportional to the number of monomers it contains:

$$(\sigma(X))^3 \propto X \tag{3}$$

It is then assumed that the distribution of β particle masses is normal, thereby, specifying the number average degree of polymerization of the β particles, $\bar{X}_n$, and their average size, $\bar{\sigma}$.

After choosing the simple units, the density profiles of the random reference polymers are calculated by solving an integrodifferential equation coupled to a stochastic differential equation, as previously described. If the simple units are linear chains, interactions at the mean-field level are included using a Flory−Huggins approach. If they are β particles, it is assumed they have no internal structure. A limit has to be placed on the density to take into account repulsions. This density, ρ_0, is given by

$$\rho_0 = \kappa\bar{\sigma}^{-3} \tag{4}$$

where κ is to be obtained from a fit to experiment (although it can in principle be obtained from independent experiments[16]). For a single unit of density profile given by eq 4, $R_g = \sqrt{3}\sigma$. This determines the constant of proportionality in eq 3. The final outcome is the dependence of the total degree of polymerization (or equivalently total molecular weight) on R_g. This is compared to he experimental dependence of weight-average molecular weight, $\bar{M}_w(R_g)$.

For the case when the simple unit is a linear polymer, the input independent parameter set thus consists of the "bond" length l, the persistence length τ, $\bar{X}_n$, the maximum density ρ_0 (or equivalently κ, from eq 4), and the Flory−Huggins parameter χ. In the case of β particles as simple units, we need $\bar{X}_n$, the width of the distribution of degrees of polymerization (ν), $\bar{\sigma}$, and κ. Each of these quantities can, in principle, be independently experimentally estimated.

The first approach to comparison between experimental and random reference structure is possible with the relations given above, using a plot of hydrodynamic radius against $\bar{M}_w(V_h)$. If we wish instead to use the second method, based on distributions, a little more is needed, as described fully elsewhere.[16] In summary, the reference randomly branched mass distribution is generated from the dependence of $\bar{M}_w$ on V_h, $\bar{M}_w(V_h)$, and the experimental number distribution, as

$$w_{ran}(\log V_h) = X_{tot,ran}(V_h)V_h N_{ex}(V_h) \tag{5}$$

where the subscript "ex" denotes quantities obtained from experiment, X_{tot} is the total degree of polymerization in a molecule, and $w_{ran}(\log V_h)$ is the random reference mass distribution. In the comparison of the random and experimental SEC weight distributions (to within an arbitrary normalization constant), the size reveals how close the sample being studied resembles a randomly assembled particle.

Results and Discussion

Figure 1 shows TEM images of rat liver and slipper limpet glycogens, with scale bars indicating the sizes of some typical particles; these were obtained using techniques described in detail elsewhere.[1] For both glycogens, two types of particles are visible: the smaller β particles around 20 nm in diameter,

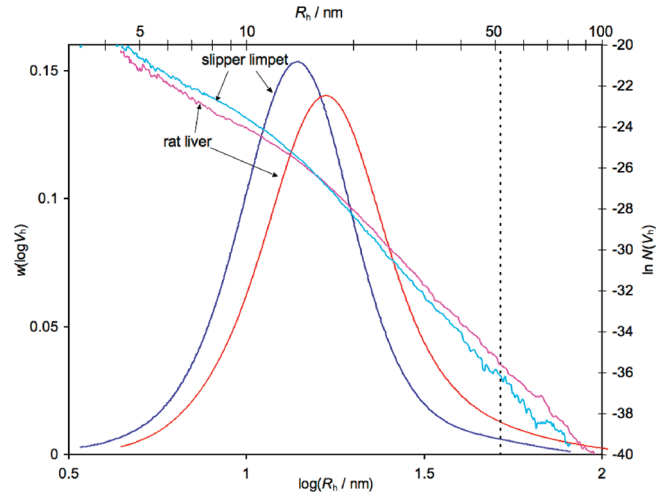

Figure 3. Number [$N(V_h)$, monotonically decreasing lines] and SEC weight [$w(\log V_h)$] distributions for slipper limpet and rat liver glycogen. Broken vertical line: upper limit of SEC calibration.

and the larger α particles made up of β particles. No free β particles are visible in the right-hand, rat liver glycogen, image. We expect to see both these particles in the SEC data, with the rat liver α particles being larger than those found in slipper limpet glycogen. For a nonglobular polymer such as glycogen, TEM and SEC sizes can only be compared semiquantitatively. Indeed, the TEM and SEC used different solvents (water and DMSO, respectively), and so the different solvents might perhaps also cause some change in size due to different behavior as the solvent is removed under vacuum for the TEM grid preparation. Both types of glycogen particles are larger in the rat liver sample than the commercial slipper limpet sample, as expected if the latter is degraded.

Figure 3 shows the number and SEC weight distributions, $N(V_h)$ and $w(\log V_h)$, for rat liver and slipper limpet glycogen, plotted as functions of R_h, together with the upper limit of calibration. The range for most of the mass of polymer is below the upper limit of calibration ($R_h \sim 50$ nm), which is also the approximate range over which shear scission in this SEC setup is negligible.[18]

The SEC weight distribution $w(\log V_h)$ does not show any remarkable features for either glycogen. However, for both glycogens, the number distribution $N(V_h)$, plotted as ln N against log R_h, shows a monotonically decreasing distribution with two distinct regions, separating at $R_h \sim 15$ nm (or ~ 30 nm in particle diameter). This is commensurate with the size gap between β and α particles, given that SEC and TEM sizes will be different, as discussed above. While the $N(V_h)$ data have potential for understanding the biosynthetic processes involved by fitting to quantitative models,[3] this is not attempted here. One reason for this is that such a fit would need to take SEC band-broadening into account, which can significantly change the shape of distributions in a way that can frustrate testing model assumptions.[30]

Figure 4 shows the weight- and number-average molecular weights of the rat liver and slipper limpet glycogen as a function of hydrodynamic radius. Although the higher molecular weights seem significantly higher than is possible to analyze for linear polymers in SEC without shear scission, it must be recalled that these glycogen polymers are hyperbranched and, thus, have a much lower size than that of a linear with the same molecular weight. At low R_h, concentration has a greater effect on the signal than molecular weight, which is the reason for there being an artifactual increase in $\bar{M}_w(V_h)$ at the lower end of the size

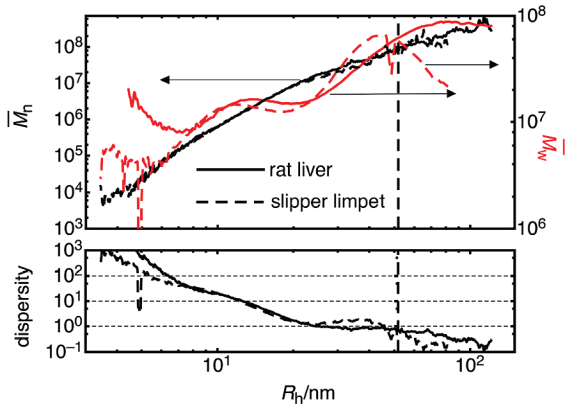

Figure 4. Number- and weight-average molecular weights, and dispersity, as functions of hydrodynamic radius for rat liver and slipper limpet glycogen. Broken vertical line: upper limit of SEC calibration.

range. The lower panel in Figure 4 shows the ratio of these two weights, that is, the dispersity $Đ$ (the term "dispersity" is that recommended by IUPAC[31] to replace terms such as polydispersity or polydispersity index). It is expected that, for randomly branched polymers, the dispersity should approach its minimum possible value, unity, as the polymers become larger.[15] Apparent dispersities less than 1 in Figure 4 are only seen outside the calibration limit and are artifactual. The expected approach to unit dispersity is thus verified experimentally. It is seen that unity is approached at about the same value of R_h as the change in slope in ln $N(V_h)$ in Figure 3: $R_h \sim 20$ nm (or ~ 40 nm diameter). Above this value, $\bar{M}_n(V_h)/\bar{M}_w(V_h) = 1$, in the range of sizes that correspond to the α particles seen in the electron micrograph. For smaller sizes characteristic of β particles, $\bar{M}_n(V_h)$ is much less than $\bar{M}_w(V_h)$: a very broad distribution of weights for each hydrodynamic radius.

The dependence of $\bar{M}_n$ on R_h, given in Figure 4, is monotonically increasing, as expected: the bigger the polymer particle, the greater its average mass. As in Figure 3, there is a change in slope at $R_h \sim 20$ nm. The dependence of $\bar{M}_w$ on R_h clearly shows two distinct regions, and the change between these regions is similar to that of the change in slope of ln $N(V_h)$ and in the dispersity. This is consistent with there being two types of particles, with the size ranges being consistent with those for α and β particles seen in the micrographs.

These data are now fitted with RBT theory, as described in the Theory section, through $\bar{M}_w(R_h)$. Figures 5 and 6 shows some of the same data as in Figure 4 for slipper limpet and rat liver glycogen, now as $R_h(\bar{M}_w)$. The fit concentrates on the region of these curves from $R_h = 6-35$ nm, a range containing most of the polymer (as shown in the SEC weight distributions, Figure 3). Each of the two regions in the $R_h(\bar{M}_w)$ curve separately show the expected growth of radius with mass. The first of these is between 6 and 9 nm radius (12−18 nm diameter) for the slipper limpet, and between 8 and 11 nm (16−22 nm diameter) for the rat liver sample, corresponding to the typical sizes of the β particles seen in Figure 1. The second ranges in radii from 22 to 35 nm for the slipper limpet and from 24 to 40 nm for the rat liver sample, corresponding to the α particles of Figure 1. Fits of RBT to both regions of the $R_h(\bar{M}_w)$ curve are shown also in Figures 5 and 6, obtained as described above, with the parameters corresponding to these fits in Tables 1 and 2. Note the two types of fit: the random assembly of linear, oligomeric chains into β particles gives the four curves labeled "oligomer RBT", and the random assembly of β particles gives the single curve labeled "β particle RBT".

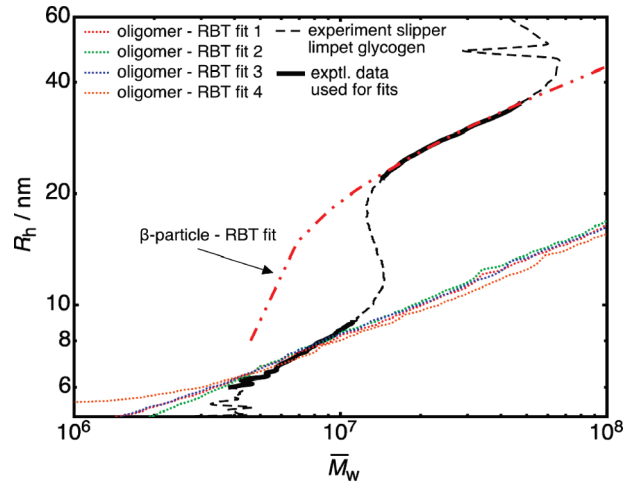

Figure 5. Experimental and modeled hydrodynamic radii (R_h) as a function of weight-average molecular weight for slipper limpet glycogen. Four different curves (dotted) are constructed by random attachment of linear chains (Table 1). A single best fit is shown for the assembly of β particles into α particles (solid curve). The regions of the experimental data used for the fits are indicated by bold curves.

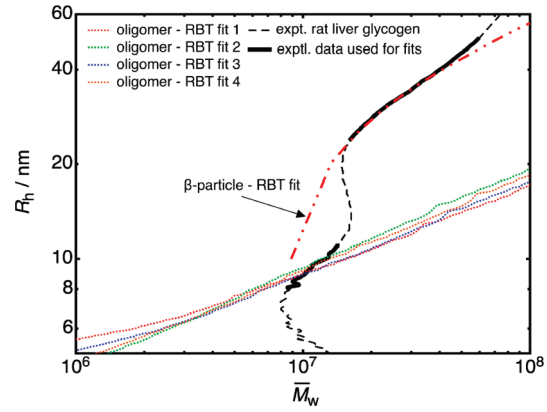

Figure 6. Experimental and modeled hydrodynamic radii (R_h) as a function of weight-average molecular weight for rat liver glycogen (see caption of Figure 5 for additional information).

Table 1. Results of Fitting RBT Based on the Random Attachment of Linear Chains to Size-Separation Data on Rat Liver and Slipper Limpet Glycogens

glycogen	fit label	$\bar{X}_n$	τ	κ	χ	$\bar{\sigma}$/nm
slipper limpet	oligomer-RBT 1	7	3	1.8	2	1.0
	oligomer-RBT 2	7	2	0.3	1.5	0.5
	oligomer-RBT 3	9	2	1	1.5	0.8
	oligomer-RBT 3	12	3	3.2	2	1.3
rat liver	oligomer-RBT 1	7	3	1.8	1.5	1.0
	oligomer-RBT 2	7	2	0.2	2	0.5
	oligomer-RBT 3	9	2	1.8	2	1.1
	oligomer-RBT 3	12	2	0.6	15	0.8

The parameter values to fit the small-R_h component are different from those used previously[16] to fit large amylopectin molecules with RBT. These earlier parameters, using the value of $\bar{X}_n$ as appropriate to glycogen (~7 rather than 17), give a significantly less compact structure than observed experimentally for the present case of glycogen, with molecular size much smaller than amylopectin: for glycogen, the R_h predicted for a given $\bar{M}_w$ is about a factor of 5 larger than experiment. To obtain accord with experiment, random-branch theory glycogen must be made more compact than that predicted from a priori estimation of the model parameters; as shown in Table 1, this

Table 2. Results of Fitting RBT Based on the Random Attachment of β Particles to Size-Separation Data on Rat Liver and Slipper Limpet Glycogens

glycogen	$\bar{X}_n$/1000	ν/1000	κ	$\bar{\sigma}$/nm
slipper limpet	28	34	0.02	4.6
rat liver	55	67	0.01	5.8

can be done in a number of ways, such as having a nonzero χ parameter. The different parametrizations leading to similar RBT $R_h(\bar{M}_w)$ dependences over the range of interest (6−10 nm) in fact give different predicted dependences for smaller R_h, but this is outside the range of observation.

The result that the "simple" RBT prediction gives a randomly branched molecule that is not as compact as experiment is unlikely to be due to a "mathematical" failure of the RBT treatment: the equations used to evaluate the structure in RBT give agreement with numerically exact simulations using the same input parameters. The inference that the RBT structure is more compact than predicted for completely randomly branched oligomers with physical parameters expected from their expected properties suggests that there may be some variation in the distribution of the two different types of glycosidic link within the polymer, that is, a nonuniform distribution of branch points. This is perhaps the simplest type of branching correlation we can imagine; it is also possible that pair or higher order correlations in the arrangement of branches is present. This is suggested in the sketches of Figure 7, which illustrates how the density (monomer units per unit volume) can increase if the branches were joined in groups rather than completely randomly; it is, however, emphasized that this is only speculative.

Figure 4 shows that the molecular weight of rat liver α particles increases more rapidly with size than do those of slipper limpet, consistent with the larger β particles in the rat liver sample. This behavior is seen also in the fit reported by Konkolewicz et al.[15] of RBT to data on a commercial glycogen.[32]

The alternative method of fitting the data with RBT is to use the experimental $N(V_h)$ to generate the randomly branched weight distribution, as in eq 5. The results for rat liver glycogen using the parameters given in Tables 1 (using the oligomer-RBT 1 parameters) and 2 are given in Figure 8. It is apparent that RBT successfully reproduces the experimental $w(\log V_h)$ using the appropriate part of the $w_{ran}(\log V_h)$ of each of the two components. This is pleasing because this method of fitting the data is not quite equivalent to that of comparing $R_h(\bar{M}_w)$ given above, because they use different distributions/dependences that are independent of each other for branched polymers: $w(\log V_h)$ and $\bar{M}_w(V_h)$. Moreover, Figure 8 suggests that the observed $w(\log V_h)$, while apparently featureless, in fact, is the sum of two randomly branched components: those made from small chains linked randomly for the smaller component, with a changeover to those made from these smaller particles themselves randomly linked to form the larger component.

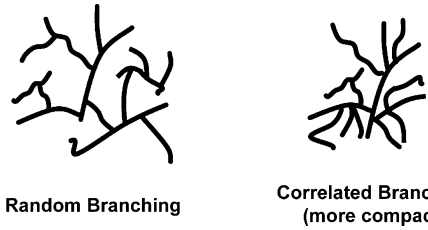

Figure 7. Sketch indicating how a correlation between branch points can result in a more compact particle.

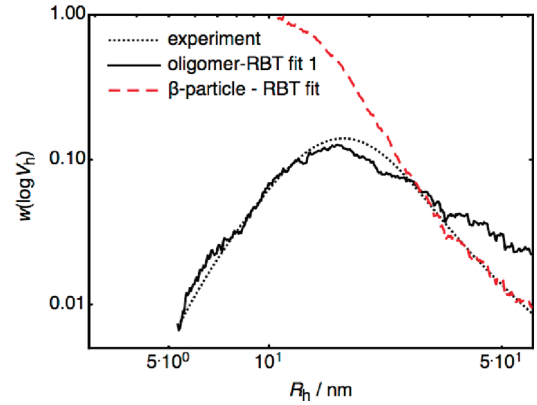

Figure 8. Experimental $w(\log V_h)$ for rat liver glycogen and the randomly branched reference function calculated as described in the text.

Table 3. Dependence of *z*-Average Particle Size of Rat Liver Glycogen in DMSO for Different Concentrations of LiBr

w/w % LiBr	*z*-average size/nm
0	103
0.5	107
5	155

The last question to be addressed is the nature of the links between β particles to form α particles: covalent or hydrogen bonding/protein−protein (weak electrostatic) forces. Table 3 shows the *z*-average particle size of the glycogen particles in DMSO with varying concentrations of LiBr. The higher LiBr concentrations disrupt strong hydrogen bonding and electrostatic interactions in starch[17] and, if these were the only binding present, would be enough to separate the β particles into the individual particles. It is seen that increasing concentrations of LiBr in fact increase the *z*-average particle size, as seen also by increasingly high ionic strength in water solutions of starch.[33] This suggests that β particles consist of particles with covalent linkages. This is consistent with the report, mentioned above, that the particles could not be separated by strong acid or reducing agent.[13]

Electron microscopy reveals no self-similarity in the structures of glycogen particles, and experimental size versus mass dependences are not a power law, in agreement with the analysis[15] of previous experiments.[32] This suggests that glycogen particles do not have a fractal structure.[31]

Conclusions

Liver glycogen has an unusual structure for a complex branched molecule because transmission electron microscopy suggests that it comprises groups of small β particles that are apparently randomly joined together to form larger α particles. This structure was investigated for native glycogen from rat liver and slightly degraded glycogen from slipper limpet by using multiple-detection SEC. These give three independent one-dimensional distributions describing different, and complementary, aspects of this complex structure. These are the number and weight distributions as functions of size (hydrodynamic volume or equivalently hydrodynamic radius), and the dependence of the weight-average molecular weight on size, $\bar{M}_w(V_h)$, together with $\bar{M}_n(V_h)$, was obtained from the same data. Note that these four dependences are inter-related,[34] and only three, say $\bar{M}_w(V_h)$, $w(\log V_h)$, and $N(V_h)$, are truly independent of each other. The size dependence of the number-average molecular

weight, $\bar{M}_n(V_h)$ can be calculated from these three independent sets of data. The observed $N(V_h)$ and $\bar{M}_w(V_h)$ suggest that there are two types of particles with different branching structures, with sizes commensurate to those inferred for the α and β particles from TEM. The use of multiple detection to provide various one-dimensional projections of the infinite-dimensional distribution function describing the structure of a branched polymer reveals features that may not be seen with the use of a single detector to provide just the weight distribution, as is common practice. It is found that the dispersity $\bar{M}_w/\bar{M}_n$ approaches unity for the larger (α) particles, as expected from theory[35] if their branching structure were random.

The size-separation data were successfully fitted using random-branching theory (RBT)[15,16] based on the premise that the polymer comprises simple units that are joined randomly. For the β-particle (smaller) component, the fit was based on assuming that the simple units are the oligomers comprising the individual branches; the α-particle (larger) component was based on the premise that the simple unit comprised β particles. The fitting to the smaller component resulted in parameter values, suggesting that the branching structure of β particles in glycogen is not fully random: there may, for example, be some sort of clustering of branches.

An examination of the dependence of the average size of the glycogen molecules dissolved in dimethylsulfoxide with increasing amounts of LiBr indicated that the binding of β particles to form α particles is not through hydrogen bonds or weak protein−protein interactions. This suggests that the bonding is covalent. There is no obvious enzymatic process to cause this. Glycogenin, glycogen synthase, glycogen branching enzyme, glycogen phosphorylase, and glycogen debranching enzyme are the important enzymes involved in glycogen synthesis and breakdown. All are essentially glucosyltransferases, in that they have the ability to transfer glucose residues to existing oligosaccharides within the glycogen particle. Given that α particles only exist in the liver in mammals, glycogen synthase is a potential candidate, because there are two genes for this enzyme, one of which is only expressed in the liver.[36] However, glycogen synthase increases glycogen chains one UDP-glucose residue at a time,[37] so how this enzyme is involved in the formation of liver α particles is unknown. Additional candidates include the branching and debranching enzymes, because they have the ability to transfer large oligosaccharide chains in one reaction step,[37] which would be required if β particles were covalently joined to form α particles.

The data given here, when combined with the random-branching theory, show that glycogen biosynthetic processes form β particles with a compact random assembly of individual branches up to some particle size range (∼30−50 nm), and in the liver, another process covalently bonds these β particles to form random clusters of α particles (as can be seen from Figure 8). It is only a combination of theory and experiment that reveals this information. A question for the future is the reason that these enzymes do not create α particles in, for example, muscle, whose glycogen comprises only individual β particles.[1]

Acknowledgment. A.A.G.-W. thanks Monash University for a fellowship. R.G.G. gratefully acknowledges the support of an Australian Research Council grant (DP0985694), D.S. acknowledges support from the National Health and Medical Research Council, and F.V. greatly appreciates the support of a postdoctoral fellowship from the Knut and Alice Wallenberg Foundation (Sweden), as well as a helpful interaction with Dr. Peter Kilz (PSS).

References and Notes

(1) Ryu, J.-H.; Drain, J.; Kim, J. H.; McGee, S.; Gray-Weale, A.; Waddington, L.; Parker, G. J.; Hargreaves, M.; Yoo, S.-H.; Stapleton, D. *Int. J. Biol. Macromol.* **2009**, *45*, 478–482.
(2) Newsholme, E. A.; Start, C. *Regulation of Metabolism*; Wiley: New York, 1974.
(3) Gray-Weale, A.; Gilbert, R. G. *J. Polym. Sci., Part A: Polym. Chem. Ed.* **2009**, *47*, 3914–3930.
(4) Kowalkowski, T.; Buszewski, B.; Cantado, C.; Dondi, F. *Crit. Rev. Anal. Chem.* **2006**, *36*, 129–135.
(5) Takeuchi, T.; Iwamasa, T.; Miyayama, H. *J. Electron Microsc.* **1978**, *27*, 31–38.
(6) Putaux, J.-L.; Buleon, A.; Borsali, R.; Chanzy, H. *Int. J. Biol. Macromol.* **1999**, *26*, 145–150.
(7) Drochmans, P. *J. Ultrastruct. Res.* **1962**, *6*, 141–163.
(8) Rybicka, K. K. *Tissue Cell* **1996**, *28*, 253–265.
(9) Shearer, J.; Graham, T. E. *Can. J. Appl. Physiol.* **2002**, *27*, 179–203.
(10) Mu, J.; Roach, P. *J. Biol. Chem.* **1998**, *273*, 34850–34856.
(11) Lomako, J.; Lomako, W. M.; Whelan, W. J. *Biochim. Biophys. Acta, Gen. Subj.* **2004**, *1673*, 45–55.
(12) Chee, N. P.; Geddes, R. *FEBS Lett.* **1977**, *73*, 164–166.
(13) Iwasama, T.; Fujisaki, A.; Takeuchi, T. *J. Electron Microsc.* **1970**, *19*, 371–380.
(14) Watts, C. J. C.; Gray-Weale, A.; Gilbert, R. G. *Biomacromolecules* **2007**, *8*, 455–463.
(15) Konkolewicz, D.; Gilbert, R. G.; Gray-Weale, A. *Phys. Rev. Lett.* **2007**, *98*, 238301/238301−238304.
(16) Gray-Weale, A.; Cave, R. A.; G.Gilbert, R. *Biomacromolecules* **2009**, *10*, 2708–2713.
(17) Schmitz, S.; Dona, A. C.; Castignolles, P.; Gilbert, R. G.; Gaborieau, M. *Macromol. Biosci.* **2009**, *9*, 506–514.
(18) Cave, R. A.; Seabrook, S. A.; Gidley, M. J.; Gilbert, R. G. *Biomacromolecules* **2009**, *10*, 2245–2253.
(19) Grubisic, Z.; Rempp, P.; Benoit, H. *J. Polym. Sci., Polym. Lett. Ed.* **1967**, *5*, 753–759.
(20) Grubisic, Z.; Rempp, P.; Benoit, H. *J. Polym. Sci., Part B: Polym. Phys.* **1996**, *34*, 1707–1714.
(21) Hamielec, A. E.; Ouano, A. C. *J. Liq. Chromatogr.* **1978**, *1*, 111–120.
(22) Kuge, T.; Kobayashi, K.; Tanahashi, H.; Igushi, T.; Kitamura, S. *Agric. Biol. Chem.* **1984**, *78*, 2375–2376.
(23) Wang, Y.; Teraoka, I.; Hansen, F. Y.; Peters, G. H.; Hassager, O. *Macromolecules* **2010**, *43*, 1651–1659.
(24) Jones, R. G.; Kahovec, J.; Stepto, R.; Wilks, E. S.; Hess, M.; Kitayama, T.; Metanomski, W. V. Compendium of Polymer Terminology and Nomenclature. In *IUPAC Recommendations 2008*; Jones, R. G., Kahovec, J., Stepto, R., Wilks, E. S., Hess, M., Kitayama, T., Metanomski, W. V., Eds.; Royal Society of Chemistry: Cambridge, 2009.
(25) Erlander, S.; French, D. *J. Polym. Sci.* **1956**, *20*, 7–28.
(26) Erlander, S. R. *Starch-Starke* **1998**, *50*, 275–285.
(27) Erlander, S. R. *Starch-Staerke* **1998**, *50*, 319–330.
(28) Rolland-Sabaté, A.; Mendez-Montealvo, M. G.; Colonna, P.; Planchot, V. *Biomacromolecules* **2008**, *9*, 1719–1730.
(29) Lin, W.; Galletto, P.; Borkovec, M. *Langmuir* **2004**, *20*, 7465–7473.
(30) van Berkel, K. Y.; Russell, G. T.; Gilbert, R. G. *Macromolecules* **2005**, *38*, 3214–3224.
(31) Gilbert, R. G.; Hess, M.; Jenkins, A. D.; Jones, R. G.; Kratochvil, P.; Stepto, R. F. T. *Pure Appl. Chem.* **2009**, *81*, 351–353.
(32) Ioan, C. E.; Aberle, T.; Burchard, W. *Macromolecules* **1999**, *32*, 7444–7453.
(33) Chiou, H.; Fellows, C. M.; Gilbert, R. G.; Fitzgerald, M. A. *Carbohydr. Polym.* **2005**, *61*, 61–71.
(34) Gaborieau, M.; Gilbert, R. G.; Gray-Weale, A.; Hernandez, J. M.; Castignolles, P. *Macromol. Theory Simul.* **2007**, *16*, 13–28.
(35) Konkolewicz, D.; Gray-Weale, A. A.; Gilbert, R. G. *J. Polym. Sci., Part A: Polym. Chem.* **2007**, *45*, 3112–3115.
(36) Nuttall, F. Q.; Gannon, M. C.; Bai, G.; Lee, E. Y. C. *Arch. Biochem. Biophys.* **1994**, *311*, 443–449.
(37) Roach, P. J. *Curr. Mol. Med.* **2002**, *2*, 101–120.

BM100074P